Chemistry–A European Journal
Research Article
doi.org/10.1002/chem.202400294
Chemistry Europe
European Chemical Societies Publishing
www.chemeurj.org

Is the E/Z Iminium Ratio a Good Enantioselectivity Predictor in Iminium Catalysis?

Matthijs A. Hellinghuizen,[a] Pietro Franceschi,[b] and Jana Roithová*[a]

Developing new enantioselective reactions is an important part of chemical discovery but requires time and resources to test large arrays of potential reaction conditions. New techniques are required to analyse many different reactions quickly and efficiently. Mass spectrometry is a high-throughput method; when combined with ion-mobility spectrometry, this technique can monitor diastereomeric reaction intermediates and thus be a handle to study enantioselective reactions. Through this technique and others, it was noted before that in the organocatalytic 1,4-addition to α,β-unsaturated aldehydes, the abundance of initial diastereomeric intermediates correlates strongly to that of the final enantiomeric products. This work determines isomeric abundance for various catalysts and aldehydes and uses it to predict the enantiomeric excess of two control reactions. The prediction matches well for one reaction but does not predict the obtained results for the second. This finding confirms that the E/Z ratio of the iminium intermediates can be used as a predictor for some reactions, but the kinetics of the following steps can dramatically change the true enantioselectivity.

Introduction

In the last few decades, organocatalysis has become an important part of asymmetric chemical synthesis,[1–6] illustrated by the 2021 Nobel Prize awarded to MacMillan and List for their roles in developing this field.[7–9] Developing new enantioselective reactions traditionally requires time, labour, and large amounts of chemicals because many reactions must be tested to optimise the yield and enantioselectivity.[10] Even though catalysts have been designed computationally, experimental confirmation is still necessary.[11] Furthermore, enantioselectivity analysis mostly relies on chiral chromatography methods,[12] increasing the time and labour costs. This can be improved upon by relying on a combination of chiral chromatography and mass spectrometry[13] and, among others, by less frequently employed methods such as VCD,[14] ECD,[15] or NMR[16] and many other techniques.[17] Instead of focusing on the products of these reactions, more efficient reaction optimisation can be achieved with knowledge of the rate- and stereo-determining steps and the intermediates involved.[18,19]

An example of this can be seen in Scheme 1, where the mechanistic explanation for the origin of enantioselectivity in the amine-catalysed 1,4-addition of nucleophiles to α,β-unsaturated aldehydes is shown.[20,21] The chiral amine-catalyst reacts with an aldehyde reactant and forms iminium intermediates. A bulky substituent on the catalyst sterically hinders the second reactant's approach to one of the two sides of the iminium intermediates. Whether the iminium ion is in the E- or Z-conformation determines which side is blocked and is, therefore, expected to largely determine the final distribution of the enantiomeric products.[22] Measuring the E/Z ratio is then a way to determine the "enantioselective potential" of a catalyst, which is defined as the predicted ee based on the E/Z ratio.

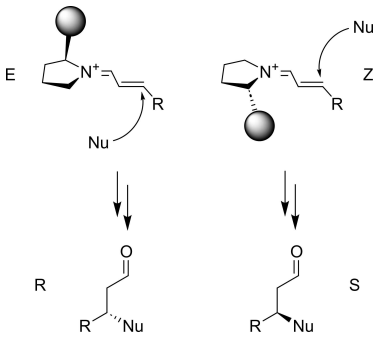

Scheme 1. A general mechanism for the enantioselective nucleophilic addition to α,β-unsaturated aldehydes. (Nu = Nucleophile).

In previous research, the E/Z ratio was determined through NMR, XRD, and DFT,[23–30] and was indeed found to be a determining factor for the enantioselectivity. However, in many cases, it is also clear that the kinetics of the following steps can change the final enantioselectivity from this expected value.[31–33] This difference between the enantioselective potential as predicted from the E/Z ratio and the "true" enantioselectivity is, therefore, an interesting aspect to investigate, as it gives insight into the role of kinetics in the following reaction steps.

[a] M. A. Hellinghuizen, J. Roithová
Institute for Molecules and Materials, Radboud University, Heyendaalseweg 135, 6525AJ Nijmegen, The Netherlands
E-mail: j.roithova@science.ru.nl

[b] P. Franceschi
Research and Innovation Centre, Fondazione E. Mach, Via Edmund Mach, 1, 38098 San Michele All'adige TN, Italy

Supporting information for this article is available on the WWW under https://doi.org/10.1002/chem.202400294

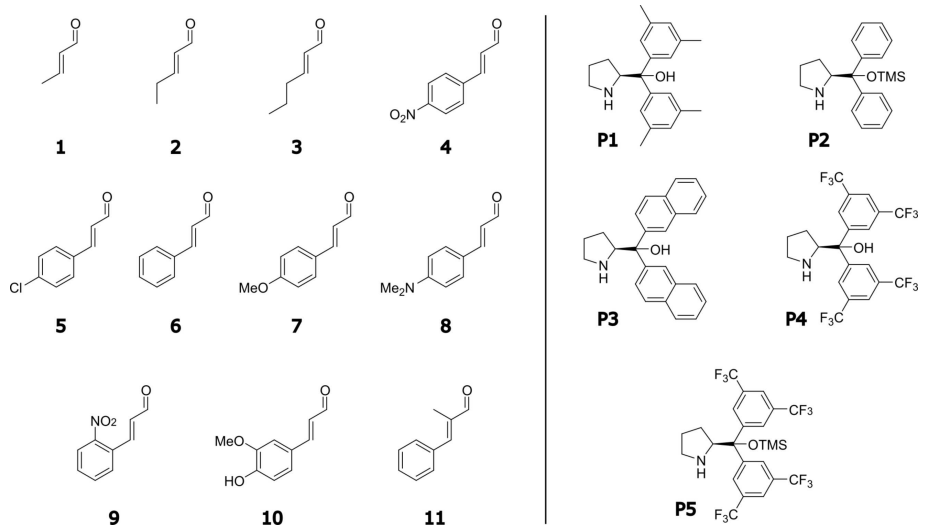

Figure 1. Aldehydes 1–11 and catalysts P1–P5 used in this research. TMS = trimethylsilyl group.

When intermediates are highly abundant, they can be investigated by NMR spectroscopy.[26,34–36] However, this is not always the case; hence, more sensitive techniques are required. Electrospray ionisation mass spectrometry (ESI-MS) has been established as a useful technique for the detection of intermediates,[37–40] because it allows parallel monitoring of different intermediates based on their m/z ratios and excels over other methods in sensitivity.[41]

Enantioselective reactions usually proceed through the reaction of a prochiral substrate with a chiral catalyst, leading to diastereomeric intermediates, which cannot be distinguished with mass analysis alone. This limitation can be overcome by Ion Mobility Separation (IMS), which separates ions according to their different shapes (collision cross sections) in the gas phase.[42–44] IMS can separate the diastereomeric intermediates in asymmetric reactions if they can be transferred to the gas phase by ESI. The combined technique of ESI-IMS-MS is a powerful tool that allows the relative abundances of isomeric intermediates to be followed over time.[45–47]

Using ESI-IMS-MS, our group previously explored the reaction pathways of the addition of cyclopentadiene to p-methoxycinnamaldehyde catalysed by a diarylprolinol silyl ether.[48] In an attempt to gain insight into the enantioselective potential, the relative amounts of E- and Z-isomers of eleven different α,β-unsaturated aldehydes with five different S-diarylprolinol catalysts (Figure 1) were determined using ESI-IMS-MS. The group of aldehydes consists of differently substituted cinnamaldehydes, along with several aliphatic α,β-unsaturated aldehydes. The prolinol catalysts differ in the substitution patterns on the aryl rings and the presence of (non−)silylated hydroxyl groups. The measured E/Z ratios were then compared to the true enantioselectivity of two organocatalysed reactions.

Results

Detection & Ion Mobilograms of Iminium Ions

ESI-MS spectra of the solutions of aldehydes 1–11 with catalysts P1–P5 showed the expected iminium ions of each aldehyde with each catalyst (Figure 2). In addition, we also detected

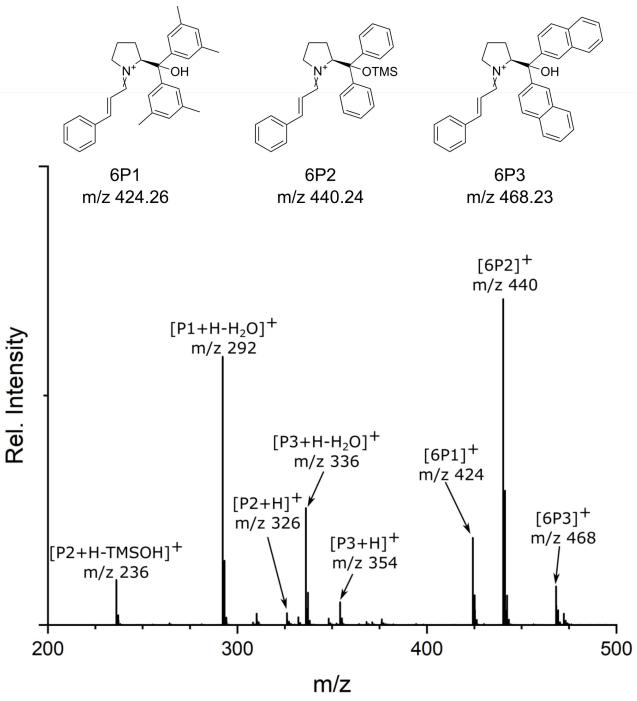

Figure 2. The ESI-MS spectrum of a solution containing aldehyde 6 with catalysts P1, P2, and P3. The iminium ions are denoted by a simplified nomenclature, indicating the combination of the aldehyde and catalyst forming the iminium ion. The listed m/z values represent the nominal masses; however, the measurements were conducted with high resolution. The ions were assigned based on the exact masses, which matched the theoretical predictions to three decimal places within the experimental error.

protonated (silyl)prolinol catalysts and ions formed by eliminating TMS-OH or H_2O from the protonated catalysts. The ion mobilograms of iminium ions 3P2 and 6P2 are shown in Figure 3. These mobilograms exhibit several peaks, indicated by the letters A–C. A and B correspond to the iminium ions with the C=N bond in the E- and Z-configurations, respectively.[48] A and B were assigned through the correlation of calculated CCSs (Collision Cross Sections)[49] and the ratio of their inverse ion mobilities ($1/K_0$) (Figure 3). C is an unidentified third isomer observed with most cinnamaldehydes. Isomer C usually has a low abundance, varying depending on the aldehyde and catalyst. In some mobilograms, an artefact caused by the fragmentation of methanol adducts is also observed, indicated by * (see supporting information).

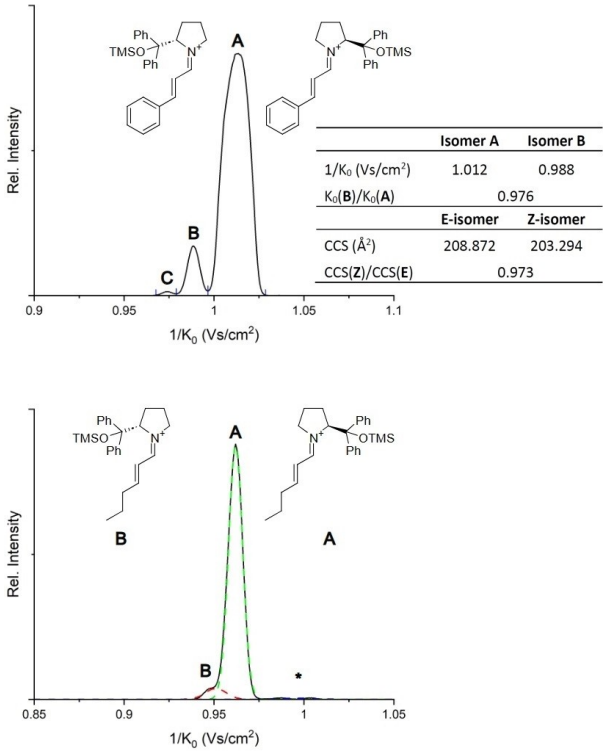

Figure 3. Mobilograms of the iminium ions 6P2 (top) and 3P2 (bottom). A - C indicate different isomers of the iminium ions. * Denotes artefact signals caused by methanol adduct fragmentation after ion-mobility separation (see supporting information). TMS = trimethylsilyl group. The green and red dotted lines in the lower mobilogram are the deconvoluted Gaussian fits of isomers A and B, respectively. The table gives the ratio of inverse mobilities of the 6P2 isomers compared to the ratio of their theoretical collision cross-sections (CCSs).

Investigation of E- and Z-Isomers

The relative abundance of E- and Z-isomers of the iminium intermediates derived from each aldehyde-catalyst combination was determined by integrating the peak areas of A, B, C, and * in the mobilograms (Table 1 and Tables S1–S5). For the smallest aldehydes (1 and 2), we did not resolve the stereoisomers of some of the iminium ions and observed only a single ion-mobility signal. Most likely, the difference in CCSs of the E- and Z-isomers is too small to separate them despite our high-resolution capability. In the rest of the mobilograms, the peaks were either separated at the baseline or it was possible to deconvolute them.

It is important to note that the isomer ratio can vary between a kinetic distribution and a thermodynamic equilibrium, and thus, it can depend on the reaction time. We have considered two sets of values. Table 1 lists the initial E/Z ratios obtained by averaging the ion intensities over the first 5 minutes immediately after the preparation of the solution. The second set is the equilibrium E/Z ratios, obtained after the ratio reached the equilibrium (5–30 min, Table S6). The catalysts strongly affected how fast the equilibrium was reached. The iminium ions with the silylated catalysts 2 and 5 quickly reached a stable signal ratio, which remained constant over time. In

Table 1. The relative peak areas of A, B, C, and * in the mobilograms of the iminium ions. The values are expressed as percentages and are rounded to the nearest whole number. These values are averaged from two duplicate measurements.

	P1				P2				P3				P4[a]				P5			
	A	B	C	*	A	B	C	*	A	B	C	*	A	B	C	*	A	B	C	*
1	100[b]	n.d.	n.d.	0	83	16	0	1	100[b]	n.d.	n.d.	0	96[b]	n.d.	n.d.	4	100[b]	n.d.	n.d.	0
2	91	9	0	0	98	2	0	0	100[b]	n.d.	n.d.	0	83	10	0	7	94	6	0	0
3	88	11	0	1	94	5	0	1	85	15	0	0	82	9	0	9	91	9	0	0
4	94	5	2	0	92	7	1	0	90	7	3	0	80	12	2	6	89	11	0	0
5	92	7	1	0	92	7	1	0	87	13	0	0	84	12	0	4	94	6	0	0
6	89	11	0	0	91	8	1	0	81	19	0	0	86	12	0	2	93	7	0	0
7	89	11	0	0	92	8	0	0	80	19	1	0	79	20	0	1	90	10	0	0
8	77	16	7	0	83	12	5	0	96	4	0	0	84	16	0	0	93	7	0	0
9	90	9	1	0	92	6	2	0	76	23	1	0	61	12	18	9	95	5	0	0
10	94	6	0	0	96	4	0	0	90	10	0	0	90	10	0	0	94	6	0	0
11	87	13	0	0	97	3	0	0	87	5	8	0	-	-	-	-	85	15	0	0

[a] Iminium ion 11P4 overlapped with the M + 1 peak of its radical cation; thus, the mobilogram could not be interpreted. [b] The E/Z isomers could not be resolved.

contrast, the iminium ions formed with the catalysts having a free hydroxyl group took longer to reach the equilibrium, although all reached equilibrium within 30 minutes. The E- to Z-isomer ratios for most of these iminium ions are slightly lower at equilibrium than at initial formation.

Reaction 1: Ene-Addition of Cyclopentadiene to α,β-Unsaturated Aldehydes

The potential of the E/Z ratio of the iminium intermediates as a predictor for enantioselectivity was tested by control reactions. The reaction of cyclopentadiene with para-methoxycinnamaldehyde 7 was chosen, as this reaction was previously studied in our group.[48] The reaction yields the ene-product (Scheme 2), as described by Gotoh et al.[50] We performed this reaction with each of the five prolinol catalysts under identical conditions and analysed the products with chiral HPLC. The final enantiomeric excess is lower than the predicted value based on the E/Z ratio of the iminium ions (Table S7 and Figure 6 below). The electron-poor prolinol catalyst P4 shows the largest deviation.

Reaction 2: Addition of Nitromethane to α,β-Unsaturated Aldehydes

As a second control experiment, the addition of nitromethane to aldehydes 4 and 5 was performed as well. This reaction was performed as reported by Gotoh et al. using catalysts P3 and P4 (Scheme 2).[51] This combination of aldehydes and catalysts was chosen because the measured E/Z ratios predict that catalyst P3 should give different enantioselectivities for aldehydes 4 and 5. Instead, catalyst P4 is predicted to give similar enantioselectivity for the two substrates. The products of this reaction were analysed by chiral HPLC to determine the enantiomeric excess. The obtained enantiomeric excess from these reactions does not correlate well with the predicted enantiomeric excess based on the E/Z ratio of the iminium ions (Table S8 and Figure 6).

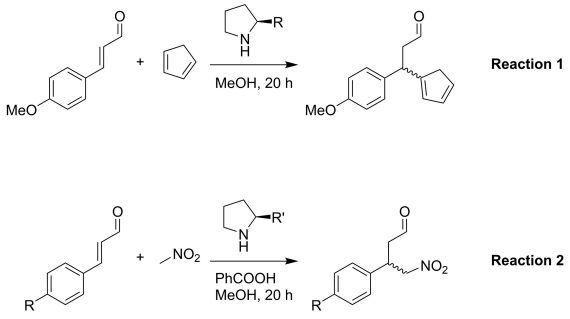

Scheme 2. The generalised reaction schemes for the ene-addition of cyclopentadiene to aldehyde 7 (top) and the addition of nitromethane to aldehydes 4 and 5 (bottom).

Discussion

Patterns in the E/Z Distribution

Table 2 shows the data from Table 1, focusing on isomers E and Z. The values give the percentage of the E-isomer in the sum of E and Z. The data are visualised in Figure 4, excluding aldehyde 1, because the isomers could not be resolved for all but one type of iminium ions. Figure 4 reveals clear patterns. In particular, the silylated catalysts P2 and P5 show, on average, a higher abundance of the E-isomer of the iminium ions and a lower diversity in the relative preference for the E-isomer than the non-silylated catalysts. This increased selectivity is probably

Table 2. The average integral areas of E-isomer as compared to the total area of E and Z.[a]

Aldehyde	P1		P2		P3		P4		P5	
1	[b]	-	84.0%	±0.9%		-		-		-
2	91.2%	±0.5%[c]	98.4%	±0.9%		-	89.4%	±0.9%	93.9%	±1.1%
3	88.6%	±0.5%	94.6%	±0.6%	84.7%	±0.7%	89.7%	±0.3%	90.5%	±0.8%
4	95.4%	±0.2%	93.2%	±0.3%	93.0%	±0.2%	87.3%	±0.8%	89.3%	±0.8%
5	92.7%	±0.1%	92.8%	±0.1%	87.5%	±0.5%	87.4%	±0.6%	94.3%	±0.1%
6	89.9%	±1.9%	91.5%	±0.4%	80.5%	±3.8%	88.1%	±1.3%	93.5%	±0.3%
7	89.3%	±0.2%	91.8%	±0.6%	80.6%	±1.3%	79.8%	±2.7%	90.3%	±0.6%
8	82.8%	±1.4%	87.8%	±0.1%	96.2%	±0.8%	84.0%	±1.2%	93.3%	±0.5%
9	91.4%	±2.0%	94.1%	±0.3%	77.1%	±0.8%	83.2%	±1.8%	95.4%	±0.1%
10	94.6%	±0.1%	96.5%	±0.1%	90.2%	±0.2%	89.7%	±1.0%	94.4%	±0.2%
11	87.4%	±1.7%	97.1%	±0.4%	94.6%	±0.0%	[d]	-	85.5%	±3.0%

[a] Cells are coloured on a spectrum from blue to red to indicate lower and higher values, respectively. [b] Grey cells indicate only a single signal was observed in the mobilogram. [c] The variance from duplicate measurements. [d] Iminium ion 11P4 overlapped with the M+1 peak of its radical cation; thus, the mobilogram could not be interpreted.

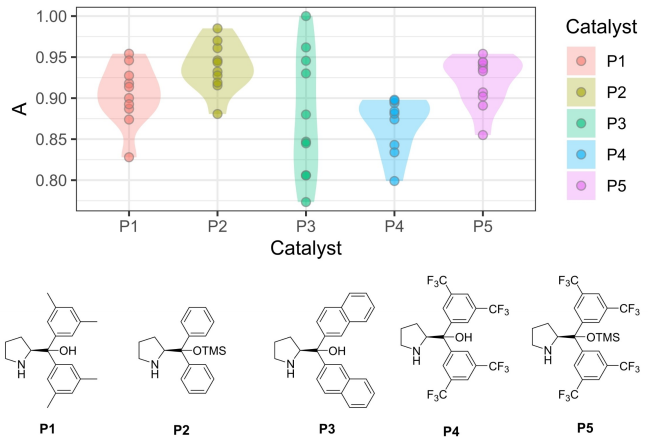

Figure 4. The amount of E isomer normalised to the total amount of E and Z for aldehydes 2–11 plotted per catalyst. Each point corresponds to a single aldehyde. The translucent violin plots show the density of the individual aldehydes. Aldehyde 1 was excluded from this analysis as it showed only a single mobility signal in all but one case. TMS = trimethylsilyl group.

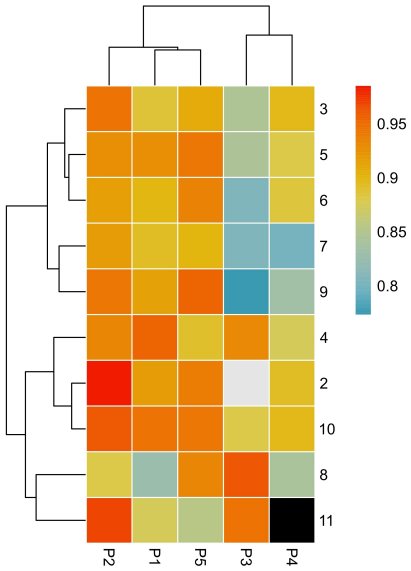

Figure 5. Each aldehyde-catalyst combination coloured by their selectivity for isomer A. The horizontal and vertical axes correspond to the catalysts and aldehydes, respectively. The aldehydes and catalysts are grouped by their similarity, shown by the dendrograms on the left and top of the graph. Aldehyde 1 was excluded from this analysis, along with iminium ion 2P3, as the isomers were unresolved in both. The mobilogram of iminium ion 11P4 could not be interpreted due to overlap with the M + 1 peak of its radical cation.

due to the additional steric bulk of the trimethylsilyl group.[30,52,53]

When comparing catalysts P1 and P3, the naphthyl-substituted catalyst has a lower E-selectivity for forming the iminium ions with most aldehydes. In particular, the abundance of Z-iminium ions formed with catalyst P3 varies greatly depending on the substitution pattern of the cinnamaldehydes. This suggests that the π-system of the naphthyl groups may play a role in stabilising the minor Z-iminium isomers. A similar effect has been observed before in organocatalysis.[31] Finally, comparing the results for fluorinated catalysts P4 and P5 with those of their approximate counterparts P1 and P2 shows that they are relatively close in their abundance for the E-isomers, with the values for the fluorinated catalysts being slightly lower. This comparison suggests that electronic changes in the catalyst are a minor factor in determining the E/Z selectivity, which is mainly determined by steric effects.

Figure 5 shows the data of Table 2 in the form of a heatmap to highlight the similarity between the aldehydes and the catalysts. Again, aldehyde 1 has been excluded from this analysis. The aldehydes and catalysts are grouped by their average similarity in selectivity for forming the E-isomer. Among the catalysts, P1, P2 and P5 show a similar response pattern with a global higher selectivity for the E-isomer. P4 and P3 are also close, lower in selectivity than the former group. Grouping the aldehydes according to the similarity of their reactions reveals no strong pattern related to the electron-withdrawing or donating groups. For example, aldehydes 4 and 10 show similar selectivity with all catalysts but are very different in their electronic properties. This suggests that the E/Z distribution is determined by a variety of factors in both the aldehyde and the catalyst and cannot be easily attributed to a single factor such as steric or electronic effects. However, as can be seen in Figure 4, the selectivity of all catalysts except P3 showed comparable diversities, meaning that the differences between the aldehydes are relatively small. Therefore, additional catalysts with a more varied response could be included in further studies to confirm the absence of such a relationship.

Comparing the Control Reactions with the Predictions

In the first control reaction, the E/Z ratio prediction correlates quite well with the obtained enantioselectivity (Figure 6), with a small drop observed in every case. We plotted the ee-

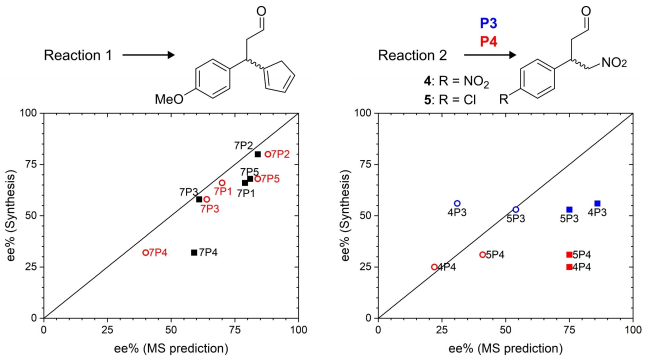

Figure 6. Left: The addition product of cyclopentadiene to aldehyde 7 and the resulting ee% plotted against the predicted ee% for each catalyst using the initial (grey squares) and equilibrium (red circles) E/Z isomer ratios. Right: The addition product of nitromethane to aldehydes 4 and 5 and the resulting ee% plotted against the predicted ee% for catalyst P3 (blue) and P4 (red). The experimental results are plotted against the initial E/Z isomer ratios (squares) and equilibrium E/Z isomer ratios (circles). In both graphs, the diagonal line corresponds to perfect agreement between prediction and reality.

predictions based on the initial and equilibrium E/Z ratios (compare black squares vs. red circles in Figure 6). Both correlate well, except for the result with catalyst P4. This catalyst performs worst, and the drop in the predicted ee when shifted towards equilibrium fits the experimental results better.

The observed small drop in enantioselectivity in Reaction 1 is expected based on the kinetics of the whole reaction sequence that we investigated in our previous research.[48] We showed that the disfavoured Z-isomer of the iminium intermediate reacts faster than the E-isomer, likely due to the larger steric strain present in the former. This decreases the enantioselectivity slightly. The steric strain, and therefore the differences in the following kinetics, will be different for each catalyst, explaining the observed variations in the decrease of enantioselectivity.

The predictions for the second control reaction do not match well with the observed results. The enantioselectivity induced by catalyst P3 is predicted to differ greatly between the two substrates. However, the obtained enantiomeric excess for each substrate is within a few percent (blue points in Figure 6). For catalyst P4, there is a major difference between the obtained enantioselectivity and the prediction obtained using the initial ratio of the formed iminium ions (red squares). These results indicate that the initial E/Z ratio of the iminium ion formation is no longer the main factor in determining the enantioselectivity. The kinetics of the following reaction steps likely play a larger role here than in the first control experiment.

The effect of the second step on the overall enantioselectivity can be analysed by a simple consideration of the reaction kinetics leading via an iminium intermediate in the steady-state approximation (Scheme 3). The simple analysis suggests that for the reactions in which the iminium intermediates react rapidly with the nucleophiles (Case 1), the rate of enamine formation depends only on k_1 in the limiting case. Accordingly, the enantioselectivity of such reactions is determined by the E/Z ratio of the iminium intermediates. This is the case for the studied cyclopentadiene addition (Reaction 1). Note that the conditions during the nucleophilic addition (Scheme 3) differ from those during our E/Z ratio measurements that proceeded in the absence of a nucleophile. Hence, the determined E/Z ratios are affected by the reverse rate constants (k_{-1}), and the limiting case is valid under the assumption that the hydrolysis of the E- and Z-iminium ions has the same rate. Alternatively, the E/Z ratios should be determined from the initial iminium ion intensities measured at the beginning of the reactions between the organocatalysts and aldehydes. The relative ion abundances should reflect the initial rates of the iminium ion formations and not be largely affected by the reverse reaction.

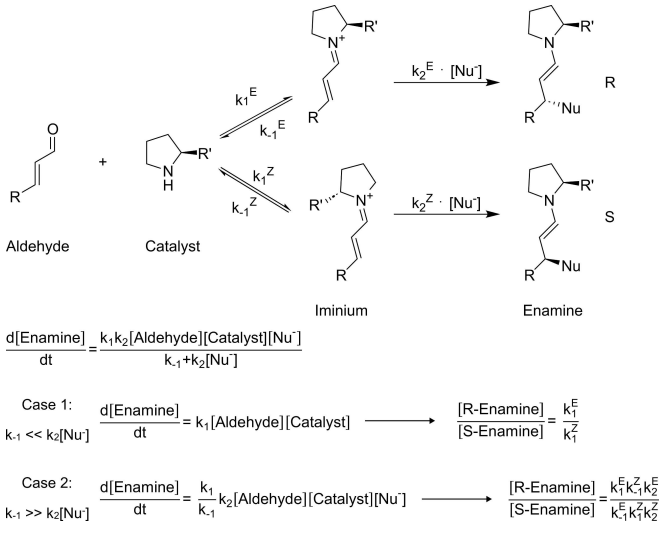

Scheme 3. A steady-state approximation for the nucleophilic addition reaction leading via the iminium intermediate and the two limiting rate equations.

In the second limiting case, the subsequent reactions of the iminium ions with nucleophiles are slow (Case 2, $k_{-1} \gg k_2$). Accordingly, the rate of enamine formation depends on k_2 and also k_{-1} (see Scheme 3). Thus, the E/Z ratio obtained from the initial rates of the iminium ions will not predict the overall enantioselectivity well.

The initial E/Z ratio does not work well for the addition of nitromethane (solid squares in Figure 6), suggesting that the nucleophile attack is slow. Therefore, we also plotted the experimental results against the predicted ee% values obtained with the E/Z isomer ratio determined at equilibrium (hollow circles in Figure 6). These values are better predictors of the outcome of Reaction 2. The low rate of the nucleophilic addition may be related to a constrained transition structure, possibly due to the hydroxyl group interacting with nitromethane. Alternatively, it could be due to a slow deprotonation of the nitromethane, resulting in a low nucleophile concentration. The latter possibility is supported by the observation that the presence of base tends to increase the enantioselectivity.[54–56]

There are also other reactions where the isomer distribution of the initial intermediate is not the determining factor for the enantioselectivity. This has been observed in enamine-based reactions, where later reaction steps determine the final enantioselectivity.[33,57]

Conclusions

In this work, we investigated several iminium ions generated from diarylprolinol catalysts and α,β-unsaturated aldehydes. We have determined the relative amounts of E- and Z-isomers of these iminium ions using the combined technique of Electrospray-Ionization Ion-Mobility-Separation Mass Spectrometry (ESI-IMS-MS). This technique allows multiple iminium ions to be measured concurrently, allowing the E/Z ratios of many catalyst-aldehyde combinations to be determined quickly.

The E- or Z-conformations of the iminium ions determine which side of the molecule is sterically hindered for a nucleophilic attack; therefore, the E/Z ratio can be taken as a measure of the potential enantioselectivity. This is especially useful as it is expected to be mostly independent of the choice of nucleophile, meaning it applies to a wide variety of reactions.

However, the E/Z iminium ratio is a good predictor only for the reactions in which the iminium ions react quickly in the

follow-up reactions with nucleophiles. We show this for the examples of the ene-reaction of cyclopentadiene with p-methoxycinnamaldehyde. Conversely, for reactions where the iminium reaction with nucleophiles is the rate-determining step, the E/Z iminium ratio fails to predict the final enantioselectivity. Such a situation was observed for the addition of nitromethane to the iminium ions.

Using the E/Z ratio as an easily measured predictor for enantioselectivity can form the basis of faster investigations into organocatalytic reactions. The tables presented in this paper could also be extended easily, adding more catalysts and aldehydes. This could allow more reaction patterns to be recognised or allow the potential of new catalysts to be quickly evaluated.

Experimental Details

Preparation of Samples

Samples Containing Catalysts P1, P2, and P3

Solutions were mixed in methanol (2 mL) with the aldehyde at a concentration of 2 mM and catalysts P1, P2, and P3 each at a concentration of 0.1 mM.

Samples Containing Catalysts P4 and P5

The iminium ions of the electron-poor catalysts P4 and P5 were consistently present at a lower intensity than the other catalysts. To get a sufficient signal for the mobilograms, these catalysts were measured separately and at a higher concentration. Solutions were mixed in methanol (2 mL) with the aldehyde at a concentration of 2 mM and catalysts P4 and P5 each at a concentration of 0.125 mM.

Samples Containing Aldehyde 11

Aldehyde 11 (α-methylcinnamaldehyde) proved to be especially unreactive towards all catalysts, presumably due to the steric hindrance of the α-methyl group. To get a sufficient signal for the mobilograms, the concentration of each catalyst was doubled. The samples were otherwise prepared identically.

Experimental Procedures

ESI-TIMS-TOF-MS

Trapped ion-mobility spectrometry-mass spectrometry experiments were performed on a TIMS-TOF MS (Bruker Daltonics Inc. Billerica, MA). Ions were generated by electrospray ionisation (ESI), with the following settings: capillary voltage 5 kV, end plate offset 500 V, dry gas 3.5 L/min, dry temperature 200 °C and nebuliser gas 0.5 bar. TIMS was operated in ultra mode at a range of 0.7–1.55 Vs/m^2 with an accumulation time of 10 ms. The RF funnels 1 and 2 were set at 400 Vpp, the multipole RF at 500 Vpp, and the deflection delta voltage was 70 V. The quadrupole ion energy was 5 eV, the transfer time 50 μs, and the pre-pulse storage time 15 μs. The samples were measured immediately after mixing, and the isomer ratio was determined based on the data collected within the first 5 minutes. The ions were assigned based on the exact masses, which matched the theoretical predictions to three decimal places.

NMR Experiments

NMR experiments were conducted on a Bruker Avance III 400 MHz spectrometer. The residual solvent peak of chloroform (δH = 7.26 ppm) was used to reference the spectra.

Chiral HPLC

Chiral HPLC Chiral HPLC analysis was performed using a Shimadzu LC-20 HPLC system. Compounds were detected using a UV detector at 215, 220 or 254 nm. To determine the enantiomeric excess of the reactions, the aldehyde products were reduced as is described in the synthetic procedures. The products were dissolved in isopropanol at an approximate concentration of 5 mg/mL.

Synthetic Procedures

Addition of Cyclopentadiene to 4-Methoxycinnamaldehyde

In methanol (1 mL), 4-methoxycinnamaldehyde (81.1 mg, 0.5 mmol, 1 eq.) and prolinol catalyst (0.05 mmol, 0.1 eq.) were dissolved. Freshly distilled cyclopentadiene (124 μL, 1.5 mmol, 3 eq.) was added and the mixture was stirred at ambient temperature and under inert atmosphere for 20 hours. The resulting mixture was purified using column chromatography (silica, EtOAc:Heptane 1:20) to yield the product. 1H NMR (400 MHz, CDCl3): δ 9.71–9.73 (0.6H, t, J = 2.1), 9.70–9.71 (0.4H, t, J = 2.1), 7.08–7.15 (2H, m), 6.80–6.87 (2H, m), 6.39–6.43 (1H, m), 6.29–6.33 (0.6H, m), 6.26–6.29 (0.4H, m), 6.23–6.26 (0.4H, m), 6.07–6.10 (0.6H, m), 4.23–4.33 (1H, m), 3.78 (3H, s), 3.02–3.07 (0.4H, m), 2.98–3.02 (0.6H, m), 2.98–3.02 (1H, m), 2.89–2.94 (0.6H, m), 2.85–2.89 (0.4H, m), 2.76–2.83 (1H, m).

Reduction and Hydrogenation of the Cyclopentadiene Product

This procedure was adapted from Gotoh et al.[50] The aldehyde product (10 mg, 0.04 mmol) obtained from the addition reaction was dissolved in methanol (1 mL) at 0 °C. Sodium borohydride (5.3 mg, 0.14 mmol) was added, and the mixture was stirred at the same temperature for 20 minutes. The reaction was quenched by adding saturated NH_4Cl, after which the product was extracted using ethyl acetate, dried over Na_2SO_4, and evaporated to dryness. The crude product was redissolved in ethyl acetate (2 mL), and 10% Pd/C was added. The mixture was then stirred overnight under the H_2 atmosphere. The reaction mixture was filtered over a celite pad and concentrated under reduced pressure. The residue was purified by preparative thin-layer chromatography (EtOAc: Heptane, 1:3) to yield the product. 1H NMR (400 MHz, CDCl3): δ 7.07 (2H, d, J = 8.6 Hz), 6.82 (2H, d, J = 8.6 Hz), 3.79 (3H, s), 3.33–3.52 (2H, m), 2.32–2.42 (1H, m), 1.86–2.12 (3H, m), 1.14–1.81 (7H, m), 0.91–1.03 (1H, m). Chiral HPLC (Phenomenex Lux Cellulose-1, 97:3 Hept:iPrOH, 35 °C, 0.5 mL/min): Tr = 40.6 min (R) and Tr = 37.6 min (S).

Addition of Nitromethane to 4-Chlorocinnamaldehyde and 4-Nitrocinnamaldehyde

This procedure was adapted from Gotoh et al.[51] In methanol (1.2 mL), 4-chlorocinnamaldehyde or 4-nitrocinnamaldehyde (0.6 mmol, 1 eq.) and prolinol catalyst (0.06 mmol, 0.1 eq.) were dissolved. After stirring for 5 minutes, nitromethane (1.8 mmol, 3 eq.) and benzoic acid (0.06 mmol, 0.1 eq.) were added. The mixture was then left to stir overnight at ambient temperature. Then, the reaction was quenched with saturated $NaHCO_3$, extracted with ethyl acetate, and dried over Na_2SO_4. After being concentrated

under reduced pressure, the crude mixture was purified using column chromatography (silica, 1:20 EtOAc:Heptane). Although each product could not be obtained in complete purity, they proved sufficiently pure after $NaBH_4$ reduction for chiral HPLC analysis.

3-(4-chlorophenyl)-4-nitrobutanal: 1H NMR (400 MHz, CDCl3): δ 9.69 (s, 1H), 7.32 (m, 2H), 7.18 (d, J = 7.6 Hz, 2H), 4.67 (m, 1H), 4.59 (m, 1H), 4.05 (q, J = 6.8 Hz, 1H), 2.92 (dd, J = 7.1, 1.0 Hz, 1H).

3-(4-nitrophenyl)-4-nitrobutanal: 1H NMR (400 MHz, CDCl3): δ 9.76 (s, 1H), 8.25 (d, J = 8.8 Hz, 2H), 7.47 (d, J = 8.7 Hz, 2H), 4.65–4.81 (m, 2H), 4.24 (q, J = 6.9 Hz, 1H), 3.05 (d, J = 7.0 Hz, 2H).

Reduction of the Nitromethane Product

The crude aldehyde (10 mg) was dissolved in methanol (1 mL) and cooled to 0 °C. Sodium borohydride (5.3 mg, 0.14 mmol) was then added and the mixture was left to stir at the same temperature for 20 minutes. The reaction was quenched by addition of saturated NH4Cl, after which the product was extracted with ethyl acetate, dried over Na_2SO_4, and evaporated to dryness.

3-(4-chlorophenyl)-4-nitrobutanol: Chiral HPLC (Chiralcel OJ, 95:5 Hept:iPrOH, 35 °C, 1 mL/min): Tr = 23.9 min (R) and Tr = 26.7 min (S).

3-(4-nitrophenyl)-4-nitrobutanol: Chiral HPLC (Chiralcel OJ, 90:10 Hept:iPrOH, 35 °C, 1 mL/min): Tr = 83.3 min (R) and Tr = 97.4 min (S).

Data Visualisation

Figures 5 and 6 were prepared in R[58] relying on ggplot2[59] and pheatmap[60] packages.

Supporting Information Summary

References cited in the Supporting Information.[50,51]

Acknowledgements

This work was supported by the Dutch Research Council (NWO – OCENW.KLEIN.348 and VI.C.192.044).

Conflict of Interests

The authors declare no conflict of interest.

Data Availability Statement

The data that support the findings of this study are openly available in Radboud Data Repository at https://doi.org/10.34973/ncrw-x871, reference number 115.

Keywords: Enantioselectivity · Iminium ions · Ion mobility separation · Mass spectrometry · Organocatalysis

[1] B. Han, X.-H. He, Y.-Q. Liu, G. He, C. Peng, J.-L. Li, *Chem. Soc. Rev.* **2021**, *50*, 1522–1586.
[2] M. Wang, L. Zhang, X. Huo, Z. Zhang, Q. Yuan, P. Li, J. Chen, Y. Zou, Z. Wu, W. Zhang, *Angew. Chem. Int. Ed.* **2020**, *59*, 20814–20819.
[3] O. García Mancheño, M. Waser, *Eur. J. Org. Chem.* **2023**, *26*, e202200950.
[4] X. Xiao, B.-X. Shao, Y.-J. Lu, Q.-Q. Cao, C.-N. Xia, F.-E. Chen, *Adv. Synth. Catal.* **2021**, *363*, 352–387.
[5] E. Reyes, L. Prieto, A. Milelli, *Molecules* **2023**, *28*, 271.
[6] G. J. Reyes-Rodríguez, N. M. Rezayee, A. Vidal-Albalat, K. A. Jørgensen, *Chem. Rev.* **2019**, *119*, 4221–4260.
[7] B. S. Donslund, T. K. Johansen, P. H. Poulsen, K. S. Halskov, K. A. Jørgensen, *Angew. Chem. Int. Ed.* **2015**, *54*, 13860–13874.
[8] D. W. C. MacMillan, *Nature* **2008**, *455*, 304–308.
[9] M. H. Aukland, B. List, *Pure Appl. Chem.* **2021**, *93*, 1371–1381.
[10] F. Vetica, F. Pandolfi, L. Pettazzoni, F. Leonelli, M. Bortolami, *Symmetry* **2022**, *14*, 355.
[11] N. Melnyk, I. Iribarren, E. Mates-Torres, C. Trujillo, *Chem. – Eur. J.* **2022**, *28*, e202201570.
[12] J. Teixeira, M. E. Tiritan, M. M. M. Pinto, C. Fernandes, *Molecules* **2019**, *24*, 865.
[13] C. C. Wagen, S. E. McMinn, E. E. Kwan, E. N. Jacobsen, *Nature* **2022**, 1–7.
[14] M. P. Mower, D. G. Blackmond, *ACS Catal.* **2018**, *8*, 5977–5982.
[15] C. Wolf, K. W. Bentley, *Chem. Soc. Rev.* **2013**, *42*, 5408–5424.
[16] S. Jang, H. Park, Q. H. Duong, E.-J. Kwahk, H. Kim, *Anal. Chem.* **2022**, *94*, 1441–1446.
[17] H.-L. Qian, S.-T. Xu, X.-P. Yan, *Anal. Chem.* **2023**, *95*, 304–318.
[18] D. G. Blackmond, *Angew. Chem. Int. Ed.* **2005**, *44*, 4302–4320.
[19] D. G. Blackmond, J. Am, *Chem. Soc.* **2015**, *137*, 10852–10866.
[20] K. L. Jensen, G. Dickmeiss, H. Jiang, Ł. Albrecht, K. A. Jørgensen, *Acc. Chem. Res.* **2012**, *45*, 248–264.
[21] C. Palomo, A. Mielgo, *Angew. Chem. Int. Ed.* **2006**, *45*, 7876–7880.
[22] M. Nielsen, D. Worgull, T. Zweifel, B. Gschwend, S. Bertelsen, K. A. Jørgensen, *Chem. Commun.* **2011**, *47*, 632–649.
[23] D. Seebach, U. Grošelj, D. M. Badine, W. B. Schweizer, A. K. Beck, *Helv. Chim. Acta* **2008**, *91*, 1999–2034.
[24] W. J. Stockerl, R. M. Gschwind, *Chem. Commun.* **2023**, *59*, 1325–1328.
[25] A. Tsybizova, M. Remeš, J. Veselý, S. Hybelbauerová, J. Roithová, J. Org, *Chem.* **2014**, *79*, 1563–1570.
[26] M. B. Schmid, K. Zeitler, R. M. Gschwind, *J. Am. Chem. Soc.* **2011**, *133*, 7065–7074.
[27] U. Grošelj, D. Seebach, D. M. Badine, W. B. Schweizer, A. K. Beck, I. Krossing, P. Klose, Y. Hayashi, T. Uchimaru, *Helv. Chim. Acta* **2009**, *92*, 1225–1259.
[28] U. Grošelj, W. B. Schweizer, M.-O. Ebert, D. Seebach, *Helv. Chim. Acta* **2009**, *92*, 1–13.
[29] U. Grošelj, A. Beck, W. B. Schweizer, D. Seebach, *Helv. Chim. Acta* **2014**, *97*, 751–796.
[30] D. Seebach, R. Gilmour, U. Grošelj, G. Deniau, C. Sparr, M.-O. Ebert, A. K. Beck, L. B. McCusker, D. Šišak, T. Uchimaru, *Helv. Chim. Acta* **2010**, *93*, 603–634.
[31] M. C. Holland, J. B. Metternich, C. Daniliuc, W. B. Schweizer, R. Gilmour, *Chem. – Eur. J.* **2015**, *21*, 10031–10038.
[32] E. H. Krenske, K. N. Houk, M. Harmata, *J. Org. Chem.* **2015**, *80*, 744–750.
[33] J. Burés, A. Armstrong, D. G. Blackmond, *Acc. Chem. Res.* **2016**, *49*, 214–222.
[34] J. Burés, A. Armstrong, D. G. Blackmond, *J. Am. Chem. Soc.* **2011**, *133*, 8822–8825.
[35] T. Naicker, K. Petzold, T. Singh, P. I. Arvidsson, H. G. Kruger, G. E. M. Maguire, T. Govender, *Tetrahedron Asymmetry* **2010**, *21*, 2859–2867.
[36] J.-L. Zhu, Y. Zhang, C. Liu, A.-M. Zheng, W. Wang, *J. Org. Chem.* **2012**, *77*, 9813–9825.
[37] I. Fleischer, A. Pfaltz, *Chem. – Eur. J.* **2010**, *16*, 95–99.
[38] P. Chen, *Angew. Chem. Int. Ed.* **2003**, *42*, 2832–2847.
[39] J.-T. Zhang, H.-Y. Wang, X. Zhang, F. Zhang, Y.-L. Guo, *Catal. Sci. Technol.* **2016**, *6*, 6637–6643.
[40] W. Schrader, P. P. Handayani, J. Zhou, B. List, *Angew. Chem. Int. Ed.* **2009**, *48*, 1463–1466.
[41] M. E. Belov, M. V. Gorshkov, H. R. Udseth, G. A. Anderson, R. D. Smith, *Anal. Chem.* **2000**, *72*, 2271–2279.
[42] M. E. Ridgeway, M. Lubeck, J. Jordens, M. Mann, M. A. Park, *Int. J. Mass Spectrom.* **2018**, *425*, 22–35.
[43] A. J. Levy, N. R. Oranzi, A. Ahmadireskety, R. H. J. Kemperman, M. S. Wei, R. A. Yost, *Anal. Chem.* **2019**, *116*, 274–281.
[44] Q. Wu, J.-Y. Wang, D.-Q. Han, Z.-P. Yao, *TrAC Trends Anal. Chem.* **2020**, *124*, 115801.

[45] A. Mollar-Cuni, L. Ibáñez-Ibáñez, G. Guisado-Barrios, J. A. Mata, C. Vicent, *J. Am. Soc. Mass Spectrom.* **2022**, *33*, 2291–2300.
[46] M. Zühlke, S. Sass, D. Riebe, T. Beitz, H.-G. Löhmannsröben, *ChemPlusChem* **2017**, *82*, 1266–1273.
[47] D. Hadavi, P. Han, M. Honing, *J. Flow Chem.* **2022**, *12*, 175–184.
[48] R. Hilgers, S. Yong Teng, A. Briš, A. Y. Pereverzev, P. White, J. J. Jansen, J. Roithová, *Angew. Chem. Int. Ed.* **2022**, *61*, e202205720.
[49] S. A. Ewing, M. T. Donor, J. W. Wilson, J. S. Prell, *J. Am. Soc. Mass Spectrom.* **2017**, *28*, 587–596.
[50] H. Gotoh, R. Masui, H. Ogino, M. Shoji, Y. Hayashi, *Angew. Chem. Int. Ed.* **2006**, *45*, 6853–6856.
[51] H. Gotoh, H. Ishikawa, Y. Hayashi, *Org. Lett.* **2007**, *9*, 5307–5309.
[52] Y. Hayashi, D. Okamura, T. Yamazaki, Y. Ameda, H. Gotoh, S. Tsuzuki, T. Uchimaru, D. Seebach, *Chem. – Eur. J.* **2014**, *20*, 17077–17088.
[53] L.-W. Xu, L. Li, Z.-H. Shi, *Adv. Synth. Catal.* **2010**, *352*, 243–279.
[54] S. Hanessian, V. Pham, *Org. Lett.* **2000**, *2*, 2975–2978.
[55] M. Yamaguchi, Y. Igarashi, R. S. Reddy, T. Shiraishi, M. Hirama, *Tetrahedron* **1997**, *53*, 11223–11236.
[56] M. Yamaguchi, T. Shiraishi, Y. Igarashi, M. Hirama, *Tetrahedron Lett.* **1994**, *35*, 8233–8236.
[57] J. Burés, A. Armstrong, D. G. Blackmond, *J. Am. Chem. Soc.* **2012**, *134*, 6741–6750.
[58] R Core Team, *R: A Language and Environment for Statistical Computing, R Foundation for Statistical Computing*, Vienna, Austria **2023**.
[59] H. Wickham, *Ggplot2*, Springer International Publishing, Cham, **2016**.
[60] R. Kolde, Pretty Heatmaps. R package version 1.0.12, **2019**, https://CRAN.R-project.org/package=pheatmap.

Manuscript received: January 23, 2024
Accepted manuscript online: June 17, 2024
Version of record online: July 30, 2024